Title
Induction of Brain Arteriovenous Malformation in the Adult Mouse

Authors
Chen, Wanqiu
Young, William L
Su, Hua

Publication Date
2014

DOI
10.1007/978-1-4939-0320-7_25

Peer reviewed

Chapter 25

Induction of Brain Arteriovenous Malformation in the Adult Mouse

Wanqiu Chen, William L. Young, and Hua Su

Abstract

Brain arteriovenous malformations (bAVM) are tangles of abnormal, dilated vessels that directly shunt blood between the arteries and veins. The pathogenesis of bAVM is currently unknown. Patients with hereditary hemorrhagic telangiectasia (HHT) have a higher prevalence of bAVM than the general population. Animal models are important tools for dissecting the disease etiopathogenesis and for testing new therapies. Here, we introduce a method that induces the bAVM phenotype through regional deletion of activin-like kinase 1 (*Alk1*, the causal gene for HHT2) and vascular endothelial growth factor (VEGF) stimulation.

Key words Arteriovenous malformation, Activin-like kinase 1, Angiogenesis, VEGF, Hereditary hemorrhagic telangiectasia, Mouse model

1 Introduction

Arteriovenous malformations (AVM) are tangles of abnormal, dilated vessels that directly shunt blood between the arteries and veins without a true capillary bed. It is a common phenotype in patients with hereditary hemorrhagic telangiectasia (HHT). The two main subtypes of HHT are as follows: (a) HHT1, caused by loss-of-function mutations in the endoglin (*ENG*), a type III transforming growth factor-beta (TGFβ) coreceptor, and (b) HHT2, caused by mutations in activin-like kinase 1 (*ALK1* or *ACVRL1*) gene, a type I TGFβ signaling receptor. Compared to the general population, the prevalence of bAVM in HHT1 (*ENG*) is 1,000-fold higher, and in HHT2 (*ALK1*), 100-fold higher (10/100,000) [1].

Brain AVM accounts for 1–2 % of all strokes [2]. The malformed vessels are fragile and prone to rupture, and rupture of bAVM can lead to intracranial hemorrhage and serious neurological disability or death. The risk of intracranial hemorrhage of bAVM is about 2–4 % per year [2]. Patients with unruptured bAVM can develop many neurological symptoms, e.g., seizures and headache. The pathogenesis of bAVM is currently unknown [3].

Richard Milner (ed.), *Cerebral Angiogenesis: Methods and Protocols*, Methods in Molecular Biology, vol. 1135,
DOI 10.1007/978-1-4939-0320-7_25,

To better understand the underlying mechanisms of bAVM formation, it is critical to establish reproducible and reliable animal models that mimic both macroscopic and microscopic morphological features of the human bAVM lesional phenotype, including large dysplastic, tangled vessels, and arteriovenous shunting.

Previous studies have shown that homozygous deletion of *Alk1* or endoglin results in embryonic lethality [4, 5]. Interestingly, induction of *Alk1* gene deletion at the adult stage leads to AVM formation only in small intestinal, pulmonary, and uterine vessels, but not in the brain [6]. Our group has previously shown that vascular endothelial growth factor (VEGF) stimulation in adult *Alk1* or *Eng* heterozygous mice results in vascular abnormalities at the capillary level [7–9], which supports the response-to-injury paradigm. Thus, other than genetic modification, environmental stimulus might also be involved in the onset of bAVM formation in adults. We have successfully induced the AVM phenotype in the adult mouse brain through regional *Alk1* deletion in combination with VEGF stimulation [10].

2 Materials

2.1 Animals

Adult $Alk1^{2f/2f}$ mice (exons 4–6 flanked by loxP sites) [11].

2.2 Viral Vectors

1. Adenoviral vector with cytomegalovirus (CMV) promoter driving Cre recombinase expression (Ad-Cre, Vector Biolabs, Philadelphia, PA, USA).
2. Control adenoviral vector with green fluorescent protein expression (Ad-GFP, Vector Biolabs).
3. Adeno-associated viral vectors expressing vascular endothelial growth factor (AAV-VEGF) packaged in AAV serotype 1 capsid [12–14].
4. Adeno-associated viral vectors expressing β-galactosidase (AAV-LacZ) [12–14].

2.3 Viral Vector Injection

1. Isoflurane.
2. 30 % oxygen/70 % nitrogen.
3. Anesthetic vaporizer and flowmeter.
4. Stereotactic frame (David Kopf Instruments, Tujunga, CA, USA).
5. Homeothermic temperature system (Harvard Apparatus, Holliston, MA, USA).
6. Hot Bead Sterilizers.
7. Rechargeable Cordless Micro Drill (Stoelting, Wood Dale, IL, USA).

2.4 Assorted Surgical Instruments

1. FS-2, 4-0 black silk suture.
2. Microdissecting tweezers.
3. McPherson-Vannas microdissecting scissors.
4. Hamilton syringe.
5. Forceps.

2.5 Latex Vessel Casting

1. 25-gauge 5-mL syringe.
2. Blue latex dye (Connecticut Valley Biological Supply Co., Southampton, MA, USA).
3. 4 % paraformaldehyde.
4. Methanol.
5. Benzyl alcohol.
6. Benzyl benzoate.
7. Microscope.

2.6 Determining Dysplasia Index

1. Fluorescein-lycopersicon esculentum-lectin (Vector Laboratory, Burlingame, CA, USA).
2. Leica CM1900 cryostat.
3. Fluorescent microscope.

3 Methods

3.1 Stereotactic Injection of Viral Vectors into the Basal Ganglia (See Note 1)

1. This protocol was approved by the Animal Care Committee of the University of California, San Francisco.
2. Following induction of anesthesia with 5 % isoflurane, 8-week-old $Alk1^{2f/2f}$ mice were placed in a stereotactic frame (David Kopf Instruments) with a mouth holder. The anesthesia was maintained with 1.5 % isoflurane.
3. A 1-cm midline skin incision at the top of the head was made to expose the sagittal suture and bregma.
4. A burr hole was drilled in the pericranium 2 mm lateral to the sagittal suture and 1 mm posterior to the coronal suture.
5. A 10-μL Hamilton syringe was slowly inserted into the left caudate nucleus at a depth of 3.0 mm under the dura (*see* **Note 2**).
6. A 2-μL viral suspension containing 2×10^7 plaque forming unit (PFU) Ad-Cre and 1 μL containing 2×10^9 genome copies (gcs) of AAV-VEGF were injected into the right basal ganglia at a rate of 0.2 μL/min using a ultramicro pump (World Precision Instruments). For the control group, Ad-GFP and AAV-LacZ were used.
7. The needle was retained in the brain for 10 min and then slowly withdrawn over a 5-min period (*see* **Note 3**).

8. The skin wound was closed with a 4-0 suture.
9. Brain sections were collected for analysis 8 weeks later (*see* **Note 4**).

3.2 Analysis

Visualizing malformed vessels in the brain is the first step to confirm the successful induction of the AVM phenotype. There are different techniques to visualize cerebral vasculature in small animals, including casting vessels with microfil [10, 15] or latex. Latex perfusion is the usual choice to display the AVM-like phenotype, since the particles in the latex dye are too big to pass through the capillaries [6]. Latex will present in the veins after intra-artery infusion when there is direct flow between arteries and veins (i.e., AV shunting, a major characteristic of AVM). Latex perfusion was first described by Coyle and Jokelainen [16] and later modified by Maeda et al. [17]. It is the liquid rubber that solidifies after the vasculature is filled.

Lesion volume measurement and dysplastic vessel index quantification (the number of vessels larger than 15 μm/200 vessels) [8–10, 18–20] are methods to evaluate the severity of the phenotype, enabling quantitative measurement of cerebrovascular abnormality, which could provide critical outcome evaluation in innovative brain vascular malformation therapies.

3.3 Vessel Casting with Latex Perfusion

1. Deep-anesthetize the mice with isoflurane. Open the abdominal and thoracic cavities and expose the heart.
2. Cut both the left and right atria. Slowly inject 1-mL blue latex dye into the left ventricle with a 25-gauge 5-mL syringe (*see* **Note 5**).
3. Remove the brain and fix with 4 % paraformaldehyde overnight.
4. Dehydrate the brain tissue using methanol series (50, 75, 95, and 100 % methanol, 24 h for each concentration).
5. Clarify the brain with benzyl alcohol/benzyl benzoate (1:1 ratio).
6. Cut the brain coronally using a razor blade. Image the brain AVM vessels under the microscope (Fig. 1).

3.4 Lesion Volume Quantification

1. After imaging the latex-perfused brain slide, rehydrate the brain tissue and snap-freeze in dry ice.
2. Coronally section the brain serially into 50-μm-thick sections using a cryostat. Section the entire brain region containing the AVM lesion.
3. Under a 5× microscope objective lens, image both the AVM lesion side and the contralateral corresponding region.
4. Quantify the latex area using NIH Image 1.63 software after binary (Fig. 2).

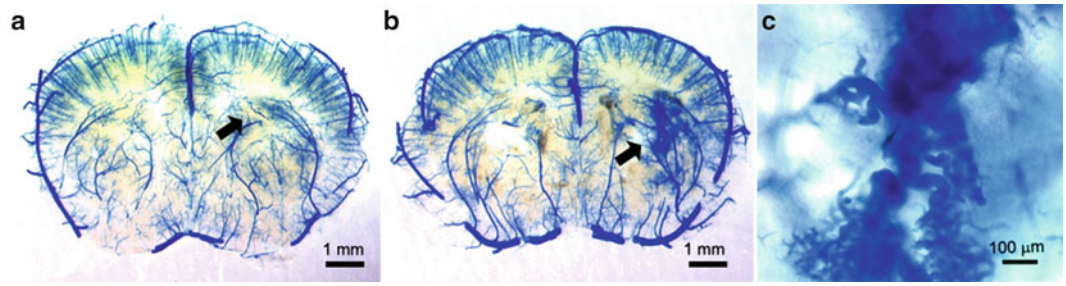

Fig. 1 Vessel casting by latex perfusion shows the AVM lesion. (**a**) No abnormal vessels were detected in the brain of wild-type mouse around the vector injection site (*arrow*). Scale bar: 1 mm. (**b**) AVM phenotype was detected around the vector injection site of 8-week-old *Alk1*$^{2f/2f}$ mouse (*arrow*). Scale bar: 1 mm. (**c**) High magnification of the injection area shows the abnormal vascular structure. Scale bar: 100 μm

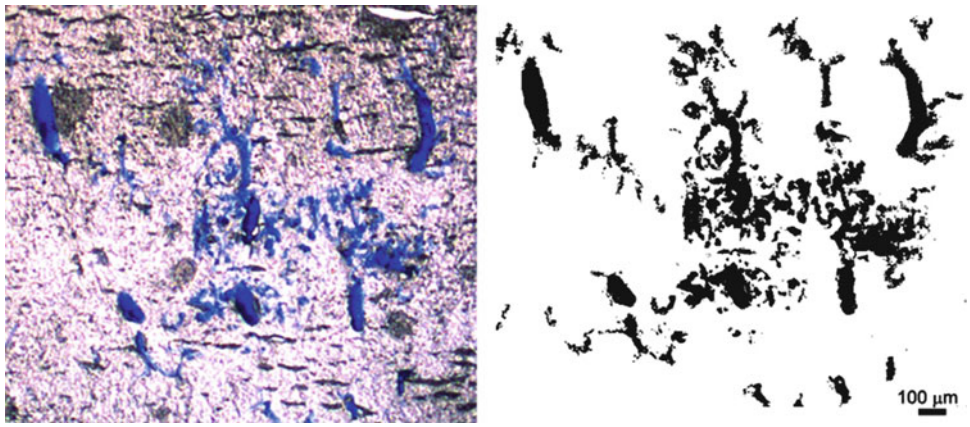

Fig. 2 An example of blue latex section image (*left*) and an image after binary (*right*). Scale bar: 500 μm

5. Based on known section thickness, estimate the volume by summing serial volumes. This method is adapted from what we have used for quantifying infarct volume in mice with middle cerebral artery occlusion (MCAO) [21].

3.5 Capillary Density and Dysplasia Index Quantification (See Note 6)

1. 8 weeks following viral injection, perfuse the mice with cold 1× PBS through the left ventricle of the heart, using a Masterflex Pump Controller (Cole Parmer Instrument, Vernon Hills, IL, USA) at 4 mL/min.
2. Harvest the brains and snap-freeze in dry ice.
3. Coronally slice the brain serially at 20-μm thickness using a cryostat.
4. Choose two sections per mouse, one mm rostral and one mm caudal of the injection site, for vessel staining using fluorescein-lycopersicon esculentum-lectin (1:200, Vector Laboratory) (Fig. 3; *see* **Note 7**).

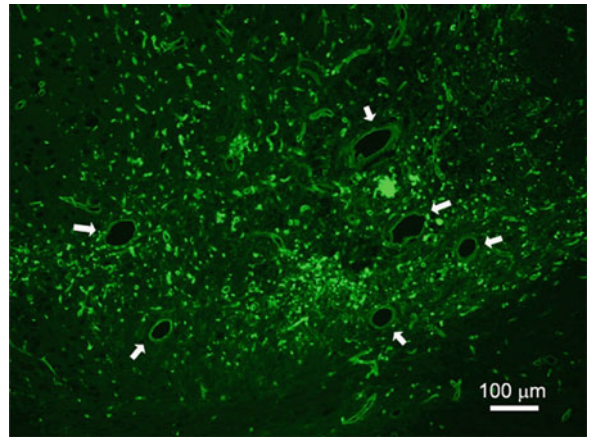

Fig. 3 Representative image of a brain section with lectin staining. *Alk1*$^{2f/2f}$ mouse received 2×10^7 PFU Ad-Cre and 2×10^9 gcs of AAV-VEGF in the basal ganglia for 8 weeks. A cluster of dysplastic vessels formed in the viral injection site (*white arrows*). Scale bar: 100 μm

5. Under a 20× microscope objective lens, capture three areas (to the right and left of and below the injection site) of each section. In each image, count total vessel number and vessels with diameter larger than 15 μm using NIH Image 1.63 software. Calculate the vascular density for each animal as the mean of the total vessel number obtained from the six images taken under 20× microscope objective lens. Calculate the dysplasia index as the number of vessels with a diameter larger than 15 μm per 200 vessels.

4 Notes

1. The vectors can also be injected into other brain regions, such as the cortex, to induce the AVM phenotype.
2. During viral injection, fix the mouse head in a horizontal position, and insert the needle perpendicularly into the surface of the dura. Needle insertion at an angle will affect the lesion location or may even inject into the brain ventricle.
3. After viral injection, it is critical to retain the needle in the brain for 10 min and then slowly withdraw the needle. Pulling the needle out too fast could lead to the virus leaking out.
4. Other than Ad-Cre-mediated regional gene deletion, *Alk1* can be conditionally deleted in adult mice, either systemically or tissue-/cell-specifically by crossbreeding *Alk1*$^{2f/2f}$ mice with transgenic mouse lines that express inducible Cre recombinase. The brain AVM phenotype can be induced in mice that have systemic/endothelial-specific *Alk1* gene deletion through intra-brain injection of AAV-VEGF.

5. For latex perfusion, make sure that the latex is fresh and that no solidified clusters have formed.
6. Vessels can also be visualized by perfusing fluorescent-labeled lectin through intravenous injection.
7. The sections can be stained with endothelial-specific antibodies, such as the anti-CD31 antibody.

Acknowledgements

This work was supported by grants from the NIH National Institute of Neurological Disorders and Stroke—R01 NS027713 (to WLY), P01 NS044155 (to WLY and HS), R21 NS070153 (to HS), and GM008440 (to WC)—and the American Heart Association, AHA 10GRNT3130004 (to HS).

References

1. Kim H, Marchuk DA, Pawlikowska L et al (2008) Genetic considerations relevant to intracranial hemorrhage and brain arteriovenous malformations. Acta Neurochir Suppl 105:199–206
2. Gabriel RA, Kim H, Sidney S et al (2010) Ten-year detection rate of brain arteriovenous malformations in a large, multiethnic, defined population. Stroke 41:21–26
3. Kim H, Su H, Weinsheimer S et al (2011) Brain arteriovenous malformation pathogenesis: a response-to-injury paradigm. Acta Neurochir Suppl 111:83–92
4. Urness LD, Sorensen LK, Li DY (2000) Arteriovenous malformations in mice lacking activin receptor-like kinase-1. Nat Genet 26: 328–331
5. Sorensen LK, Brooke BS, Li DY et al (2003) Loss of distinct arterial and venous boundaries in mice lacking endoglin, a vascular-specific TGFbeta coreceptor. Dev Biol 261:235–250
6. Park SO, Wankhede M, Lee YJ et al (2009) Real-time imaging of de novo arteriovenous malformation in a mouse model of hereditary hemorrhagic telangiectasia. J Clin Invest 119:3487–3496
7. Xu B, Wu YQ, Huey M et al (2004) Vascular endothelial growth factor induces abnormal microvasculature in the endoglin heterozygous mouse brain. J Cereb Blood Flow Metab 24:237–244
8. Hao Q, Su H, Marchuk DA et al (2008) Increased tissue perfusion promotes capillary dysplasia in the ALK1-deficient mouse brain following VEGF stimulation. Am J Physiol Heart Circ Physiol 295:H2250–H2256
9. Hao Q, Zhu Y, Su H et al (2010) VEGF induces more severe cerebrovascular dysplasia in Endoglin$^{+/-}$ than in Alk1$^{+/-}$ mice. Transl Stroke Res 1:197–201
10. Walker EJ, Su H, Shen F et al (2011) Arteriovenous malformation in the adult mouse brain resembling the human disease. Ann Neurol 69:954–962
11. Park SO, Lee YJ, Seki T et al (2008) ALK5- and TGFBR2-independent role of ALK1 in the pathogenesis of hereditary hemorrhagic telangiectasia type 2 (HHT2). Blood 111:633–642
12. Su H, Lu R, Kan YW (2000) Adeno-associated viral vector-mediated vascular endothelial growth factor gene transfer induces neovascular formation in ischemic heart. Proc Natl Acad Sci U S A 97:13801–13806
13. Su H, Huang Y, Takagawa J et al (2006) AAV serotype-1 mediates early onset of gene expression in mouse hearts and results in better therapeutic effect. Gene Ther 13:1495–1502
14. Shen F, Su H, Liu W et al (2006) Recombinant adeno-associated viral vector encoding human VEGF165 induces neomicrovessel formation in the adult mouse brain. Front Biosci 11:3190–3198
15. Walker EJ, Shen F, Young WL et al (2011) Cerebrovascular casting of adult mouse for 3D imaging and morphological analysis. J Vis Exp (57): e2958
16. Coyle P, Jokelainen PT (1982) Dorsal cerebral arterial collaterals of the rat. Anat Rec 203:397–404
17. Maeda K, Hata R, Hossmann KA (1998) Differences in the cerebrovascular anatomy of C57black/6 and SV129 mice. Neuroreport 9:1317–1319

18. Choi EJ, Walker EJ, Shen F et al (2012) Minimal homozygous endothelial deletion of Eng with VEGF stimulation is sufficient to cause cerebrovascular dysplasia in the adult mouse. Cerebrovasc Dis 33:540–547
19. Choi EJ, Walker EJ, Degos V et al (2013) Endoglin deficiency in bone marrow is sufficient to cause cerebrovascular dysplasia in the adult mouse after vascular endothelial growth factor stimulation. Stroke 44:795–798
20. Chen W, Guo Y, Walker EJ et al (2013) Reduced mural cell coverage and impaired vessel integrity after angiogenic stimulation in the *Alk1*-deficient brain. Arterioscler Thromb Vasc Biol 33:305–310
21. Shen F, Walker EJ, Jiang L et al (2011) Coexpression of angiopoietin1 with VEGF increases the structural integrity of the blood-brain barrier and reduces atrophy volume. J Cereb Blood Flow Metab 31:2343–2351